

Viscosity of Aqueous KCl Solutions in the Temperature Range 25–150 °C and the Pressure Range 0–30 MPa

Clifford E. Grimes, Joseph Kestin,* and H. Ezzat Khalifa

Division of Engineering, Brown University, Providence, Rhode Island 02912

New experimental data on the viscosity of aqueous KCl solutions are reported. The data cover the temperature range 25–150 °C, the pressure range 0–30 MPa, and the concentration range 0–4.4 *m*. The experimental values have an estimated accuracy of $\pm 1\%$ over the entire range of pressure, temperature, and concentration. The viscosity has been correlated as a function of pressure, temperature, and concentration. The paper also provides a correlation for the density of KCl solutions in terms of pressure, temperature, and concentration.

1. Introduction

The rapidly growing interest in the development of geothermal energy has created a need for reliable data on the thermodynamic and transport properties of geothermal brines. A typical geothermal brine will be a complex aqueous solution of sodium chloride, potassium chloride, calcium chloride, etc. In some areas, the geothermal brine may contain as much as 30% by weight total dissolved solids, mostly sodium and potassium chloride.

A careful search of the available literature (18) failed to reveal reliable data on the viscosity of even the most common aqueous solutions, such as those of sodium chloride, especially over extended ranges of pressure, temperature, and concentration. The present paper is the third in a series (8, 9) providing reliable experimental data on the viscosity of aqueous solutions of interest in the geothermal energy field. In the first paper (9) we presented a detailed description of the apparatus and the measuring technique as well as the results of measurements of the viscosity of water in the temperature range 10–150 °C and the pressure range 0–30 MPa. In the second paper we reported our measurements of the viscosity of sodium chloride solutions in the temperature range 20–150 °C, the pressure range 0–30 MPa, and over a concentration range extending to near saturation (0–5.5 *m*). Our work on NaCl constitutes the only study in which such wide ranges were covered simultaneously, especially the pressure range.

In this paper we report our measurements of the viscosity of aqueous KCl solutions in the temperature range 25–150 °C, the pressure range 0–30 MPa, and the concentration range 0–4.4 *m*. Again we note that these are the first measurements to combine the preceding ranges of pressure, temperature, and concentration.

2. Experimental Procedure

The measurements were performed in our oscillating-disk viscometer which was described in detail in our previous papers (7, 9, 11). The theory of the instrument and the experimental procedure were also given there. Owing to the corrosive nature of the fluids of interest, we found it necessary to change the oscillating disk and the gripping jaws for the strand. The characteristics of the new oscillating system are given in Table I.

The viscometer was calibrated in the usual manner (8, 9) using distilled water as the calibrating medium. The edge-

Table I. Characteristics of the Oscillating System

radius of the oscillating disk, R	33.99 ₂ mm
thickness of the oscillating disk, d	3.29 ₇ mm
moment of inertial of the oscillating system, I	5609 ₈ g mm ²
separation between disk and fixed plates, b	2.93 ₆ mm
period in vacuo at 25 °C, T_0	16.722 s
decrement in vacuo at 25 °C, Δ_0	0.3×10^{-4}

Table II. Schedule of Measurements

solu- tion no.	molal concn	isotherms, °C
1	0.5027	27.0, 36.0, 43.0, 66.0, 77.5, 106.0, 146.5
2	1.4984	24.5, 35.5, 44.5, 60.0, 79.5, 114.0, 148.0
3	2.5039	26.5, 35.5, 46.0, 60.0, 79.5, 106.0, 150.0
4	3.5010	25.0, 34.0, 35.0, 44.5, 59.5, 79.0, 111.5, 150.5
5	4.3925	26.0, 36.0, 45.0, 60.0, 79.0, 101.0, 148.5

correction factor (10, 13) has been correlated as a function of the boundary layer thickness δ by

$$C = 1.000 + 0.4085 \times 10^{-1}(\delta/\text{mm}) + 0.9365 \times 10^{-1}(\delta/\text{mm})^2 - 0.3767 \times 10^{-1}(\delta/\text{mm})^3 \quad (1)$$

in which

$$\delta = (\mu T_0 / 2\pi\rho)^{1/2} \quad (2)$$

with the viscosity, μ , and the density, ρ , of water taken from ref 12 and 6, respectively. Figure 1 depicts the edge-correction factor for the present oscillating system. The solid line is that represented by eq 1.

During the course of these measurements the viscometer had to be opened, cleaned, and realigned several times. After each such operation, the calibration of the viscometer was checked to find out whether the handling of the suspension system had resulted in any significant changes in it. The results of these checks are shown graphically in the deviation plot of Figure 2. It can be seen that the checkpoints deviate randomly from the original calibration, eq 1, and that the maximum deviation is only 0.3% which is of the same order of magnitude as the estimated precision of the system (9).

The viscosity was measured at five concentrations and over the nominal temperature range 25–150 °C and the nominal pressure range 0–30 MPa. We measured the viscosity along a total of seven isotherms per concentration, each comprising a minimum of seven pressure points. A point is the average of at least two independent measurements. Table II contains a summary of the scheme of measurements.

3. Density

The viscosity and density of a liquid are closely coupled in the working equations of the oscillating-disk viscometer (10, 13). To a first order of approximation, in our present arrangement

$$\Delta \sim (\rho\mu)^{1/2} \quad (3)$$

where Δ is the logarithmic decrement of the damped oscillations of the disk. This shows that the density of the liquid must be

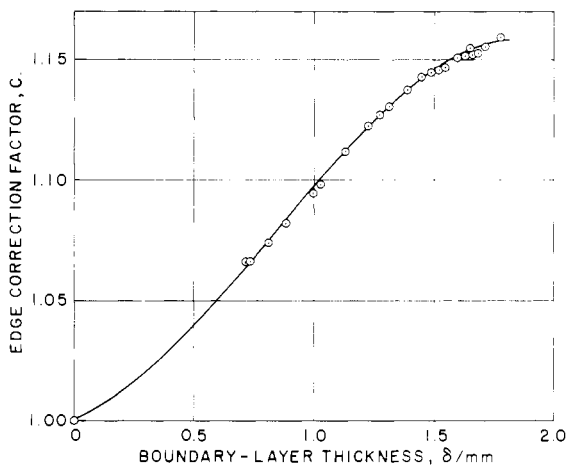


Figure 1. The edge-correction factor for the viscometer.

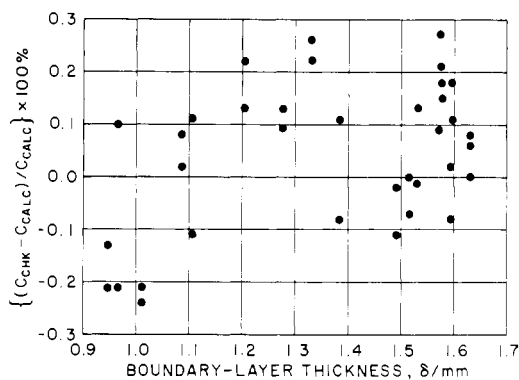


Figure 2. Comparison between the calibration check points and the correlation given by eq 1.

Table III. The Coefficients d_{ij} in Eq 5

j	$i=0$	$i=1$	$i=2$
0	1.002×10^3	0.472×10^2	-1.73
1	-0.168	-0.537×10^{-1}	-0.615×10^{-2}
2	-0.248×10^{-2}	0.128×10^{-3}	0.112×10^{-3}

very accurately known in order to determine the viscosity with a reasonable accuracy. Unfortunately, accurate values of the density of KCl solutions are not available over the pressure-temperature-concentration domain of interest in the present investigation (17). In particular, the effect of pressure on the density of KCl solutions has rarely been studied; the only source we could locate is a paper by Egorov et al. (2). As for the density at low pressure, the most extensive work is the compilation of Potter and Brown (17) which is based on a large number of sources of data.

We have, therefore, developed a correlation for the density of aqueous KCl solutions, $\rho = \rho(P, T, c)$, in which the pressure effect was taken as a linear factor derived from the data of Egorov et al. (2).

$$\rho(P, T, c) = \rho^0(T, c)[1 + \alpha(T, c)P] \quad (4)$$

The hypothetical zero-pressure density function, $\rho^0(T, c)$ was obtained from a least-squares fit of the compiled data of Potter and Brown (17) over the full range of concentration and over the temperature range 20–150 °C. Thus

$$\rho^0(T, c)/(\text{kg}/\text{m}^3) = \sum_{i=0}^2 \sum_{j=0}^2 d_{ij}(c/m)(T/^\circ\text{C})^j \quad (5)$$

in which $m = 1$ mol/kg of H_2O . The coefficients d_{ij} are given in Table III. The above correlation reproduces the compiled

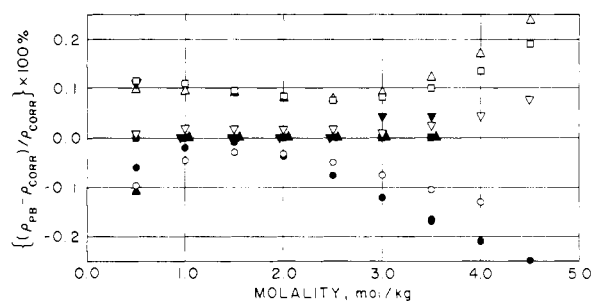


Figure 3. Comparison between the densities compiled by Potter and Brown (17) and the correlation: O, 0 °C; □, 25 °C; △, 50 °C; ▽, 75 °C; ●, 100 °C; ■, 125 °C; ▲, 150 °C; ▼, 175 °C.

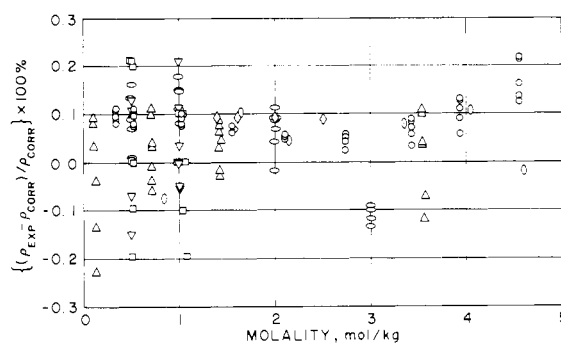


Figure 4. Comparison between our density correlation and experimental results: O, ref 5; △, ref 14; ▽, ref 3; □, ref 1; ◇, ref 21; 0, ref 4; ○, ref 15.

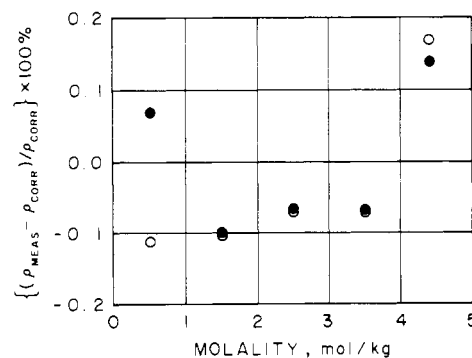


Figure 5. Comparison between the density check measurements at room temperature and the correlation: O, before measuring viscosity; ●, after measuring viscosity.

Table IV. The Coefficients a_{ij} in Eq 6

j	$i=0$	$i=1$	$i=2$
0	0.489	-0.744×10^{-1}	0.755×10^{-2}
1	-0.280×10^{-2}	0.132×10^{-2}	-0.176×10^{-3}
2	0.189×10^{-4}	-0.767×10^{-5}	0.104×10^{-5}

data (17) to within a standard deviation of $\pm 0.07\%$ and a maximum deviation of 0.23%. Figure 3 contains a comparison between the correlation and compiled data. Figure 4 depicts the differences between the correlation of eq 5 and a large set of primary experimental results (1, 3, 4, 5, 14, 15, 21). The correlation agrees with the experimental results to within a standard deviation of $\pm 0.2\%$, which is compatible with the uncertainty in the compiled values (17).

The pressure factor $\alpha(T, c)$ is expressed by the double polynomial

$$\alpha(T, c)/(\text{GPa})^{-1} = \sum_{i=0}^2 \sum_{j=0}^2 a_{ij}(c/m)(T/^\circ\text{C})^j \quad (6)$$

The coefficients a_{ij} are given in Table IV.

Table V. Viscosity of KCl Solution No. 1, $c = 0.5027 m$

P , MPa	μ , $\mu\text{Pa s}$	P , MPa	μ , $\mu\text{Pa s}$
at 27.0 °C		at 36.0 °C	
0.10	860	0.10	717
3.55	859	10.65	716
10.58	858	17.61	717
17.48	858	24.37	717
23.82	858	30.92	718
31.27	856	5.48	718
13.89	857	0.10	717
0.10	858		
at 43.0 °C		at 66.0 °C	
0.10	629	0.10	439
10.65	631	10.51	441
17.41	632	17.55	443
24.23	634	24.30	446
31.27	635	31.13	446
5.34	631	5.55	442
0.10	630	0.10	440
at 77.5 °C		at 106.5 °C	
0.65	376	1.27	275
10.44	380	10.31	278
17.34	380	17.34	279
24.30	381	24.23	281
31.20	383	31.27	283
5.69	377	6.03	276
0.93	376	0.93	275
at 146.5 °C			
1.96	197		
10.79	198		
17.61	201		
24.37	203		
31.27	204		
5.48	198		
0.85	197		

The density of the KCl solutions used in the present investigation was measured at room temperature and atmospheric pressure by means of a precision pycnometer, both before and after the measurement of viscosity. The measured densities are compared with our correlation in Figure 5; it can be seen that all the deviations are within the quoted uncertainty of the correlation, i.e., $\pm 0.2\%$.

4. Viscosity

Tables V–IX contain the experimental values of the viscosity of the five KCl solutions given in Table II. The tabulated values include check measurements taken on the decompression leg of a pressure cycle and on the cooling leg of a temperature cycle. The reported values have been adjusted to nominal temperatures by means of a small linear correction obtained from a piecemeal Arrhenius fit of our experimental results, i.e., by

$$\mu \approx A_i \exp(B_i/T) \quad (7)$$

in which optimum values of the constants A_i and B_i were calculated for two or more temperature intervals. The results are also shown graphically in Figures 6–10, which are included in the microfilm edition of this paper.

The estimated uncertainty in these measurements is one of $\pm 1\%$ —somewhat higher than the corresponding value for NaCl solutions ($\pm 0.5\%$) quoted in ref 8. This is attributed to two factors: (i) the uncertainty in the density of KCl solutions is higher than that for NaCl and (ii) the KCl solutions are more corrosive than the NaCl solutions. The interaction of the solutions with the viscometer vessel and internal parts may have resulted in local changes in the properties of the solution which affected the viscosity values. It is worth mentioning that although these

Table VI. Viscosity of KCl Solution No. 2, $c = 1.4984 m$

P , MPa	μ , $\mu\text{Pa s}$	P , MPa	μ , $\mu\text{Pa s}$
at 24.5 °C		at 35.5 °C	
0.10	905	0.10	738
10.65	905	10.44	739
17.24	906	17.41	739
24.37	906	24.44	741
30.99	906	31.20	742
5.27	905	5.27	737
0.10	904	0.10	737
at 44.5 °C		at 60.0 °C	
0.10	631	0.10	498
10.44	633	10.38	500
17.61	634	17.48	503
24.30	636	24.16	504
31.20	638	31.27	505
5.48	631	5.48	499
0.10	631	0.10	498
at 79.5 °C		at 114.0 °C	
0.79	390	1.41	277
10.24	393	10.31	279
17.68	395	17.27	281
24.16	397	23.65	283
29.47	398	31.13	285
5.48	391	5.96	278
0.93	391	0.93	277
at 148.0 °C			
1.62	214		
10.44	216		
17.55	219		
24.23	220		
1.76	215		

Table VII. Viscosity of KCl Solution No. 3, $c = 2.5039 m$

P , MPa	μ , $\mu\text{Pa s}$	P , MPa	μ , $\mu\text{Pa s}$
at 26.5 °C		at 35.5 °C	
0.10	888	0.10	761
10.44	889	10.65	763
17.55	890	17.47	763
24.23	891	24.23	765
30.99	892	31.13	765
5.20	889	5.34	760
0.10	888	0.10	759
at 46.0 °C		at 60.0 °C	
0.10	643	0.10	525
10.72	644	10.79	528
17.48	646	17.27	530
24.23	647	24.30	531
30.85	650	31.20	533
5.48	644	5.61	526
0.10	640	0.10	525
at 79.5 °C		at 106.0 °C	
0.79	414	1.14	319
10.31	416	10.51	322
17.48	419	17.41	324
24.30	421	24.23	326
31.13	423	30.99	327
5.20	415	5.07	321
0.93	413	0.86	320
at 150.0 °C			
0.79	230		
1.14	230		
10.65	233		
17.55	234		
31.06	237		
24.79	236		
5.89	231		
1.27	231		

Table VIII. Viscosity of KCl Solution No. 4, $c = 3.5010\text{ m}$

P, MPa	$\mu, \mu\text{Pa s}$	P, MPa	$\mu, \mu\text{Pa s}$
at 25.0 °C		at 34.0 °C	
0.10	932	0.10	798
10.48	934	10.72	800
17.55	935	17.61	803
24.34	937	24.37	805
31.06	939	31.20	807
17.78	937	17.75	803
5.14	934	5.20	801
0.10	933	0.10	799
at 35.0 °C		at 44.5 °C	
0.10	793	0.10	686
10.58	796	10.58	690
17.55	798	17.61	691
24.51	800	24.37	693
31.20	802	31.20	696
5.41	795	5.41	687
0.10	794	0.10	686
at 59.5 °C		at 79.0 °C	
0.10	557	1.00	442
10.65	560	10.44	444
17.61	561	17.61	445
24.37	563	24.30	447
31.13	566	31.13	450
5.41	557	17.75	445
0.10	556	5.41	442
		1.00	441
at 111.5 °C		at 150.5 °C	
0.79	326	1.00	247
10.31	328	10.44	250
17.48	330	17.34	251
24.37	332	24.10	253
31.20	334	30.92	255
18.24	330	18.24	252
5.62	327	5.62	249
0.86	326	1.21	248

Table IX. Viscosity of KCl Solution No. 5, $c = 4.3925\text{ m}$

P, MPa	$\mu, \mu\text{Pa s}$	P, MPa	$\mu, \mu\text{Pa s}$
at 26.0 °C		at 36.0 °C	
0.10	950	0.10	805
10.51	952	10.44	809
17.27	954	17.41	811
23.41	958	24.30	813
30.78	959	31.20	816
5.41	951	5.48	807
0.10	949	0.10	805
at 45.0 °C		at 60.0 °C	
0.10	705	0.10	579
10.44	709	10.31	582
17.55	711	17.48	584
24.37	713	24.30	586
31.13	715	31.13	588
5.48	707	17.92	584
0.10	706	5.41	581
		0.10	579
at 79.0 °C		at 101.0 °C	
0.79	466	0.72	379
10.38	470	10.10	381
17.55	471	17.75	384
24.30	474	24.30	386
31.20	476	31.13	387
17.96	472	18.10	384
5.48	468	5.55	381
1.07	466	1.00	380
at 148.5 °C			
0.58	267		
10.44	268		
17.48	271		
24.30	272		
31.20	274		
18.44	271		
5.69	268		
0.93	266		

changes may have affected the viscosity of the solutions, they had a negligible effect on the density as was indicated by the absence of any significant effects on the densities of samples taken from the viscometer after the completion of the measurements.

5. Analysis and Correlation of Present Results

The experimental results were analyzed and correlated in three stages. First the values along an isotherm were correlated as a function of pressure by means of a linear expression.

$$\mu(T, c, P) = \mu^0(T, c)[1 + \beta(T, c)P] \quad (8)$$

Then the zero-pressure viscosity, $\mu^0(T, c)$, was correlated in terms of temperature and concentration by an expression of the form

$$\mu^0(T, c) = \mu^0(T, 0)[1 + \sum_{i=0}^2 \sum_{j=0}^2 f_{ij}(c/m)^{i+1}(T/^\circ\text{C})^j] \quad (9)$$

In this expression $\mu^0(T, 0)$ represents the viscosity of pure water at low pressure, $\mu_w^0(T)$. Its values can be obtained from the correlation of Kestin, Sokolov, and Wakeham (12); namely

$$\log [\mu_w^0(T)/\mu_w^0(20^\circ\text{C})] = (20 - T/^\circ\text{C}) \times [1.2378 - 1.303 \times 10^{-3}(20 - T/^\circ\text{C}) + 3.06 \times 10^{-6}(20 - T/^\circ\text{C})^2 + 2.55 \times 10^{-8}(20 - T/^\circ\text{C})^3]/(96 + T/^\circ\text{C}) \quad (10)$$

The viscosity of water at 20 °C, $\mu_w^0(20^\circ\text{C}) = 1002 \mu\text{Pa s}$, is that obtained by Swindells et al. (20). The coefficients f_{ij} of eq

Table X. Optimum Values of the Coefficients f_{ij} in Eq 9

j	$i = 0$	$i = 1$	$i = 2$
0	0.113×10^{-1}	0.537×10^{-3}	0.436×10^{-6}
1	-0.235×10^{-1}	0.525×10^{-3}	-0.230×10^{-5}
2	0.450×10^{-2}	-0.868×10^{-4}	0.344×10^{-6}

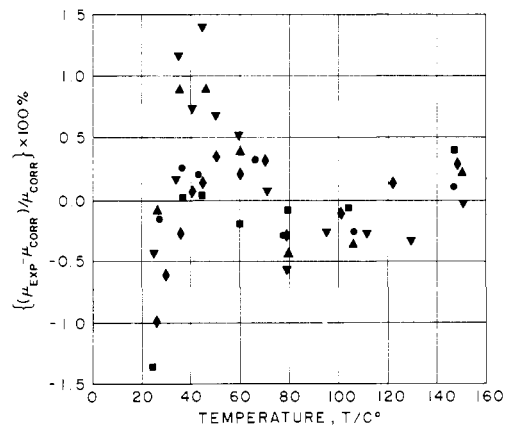


Figure 11. Comparison between the present experimental results and the correlation $\mu^0(T, c)$ (eq 9): ●, $c = 0.5027\text{ m}$; ■, $c = 1.4984\text{ m}$; ▲, $c = 2.5039\text{ m}$; ▼, $c = 3.5010\text{ m}$; ◆, $c = 4.3925\text{ m}$.

9 are given in Table X. Equation 9 reproduces the experimental low-pressure values to within a standard error of $\pm 0.5\%$; the maximum absolute deviation being 1.4% as shown in the deviation plot of Figure 11.

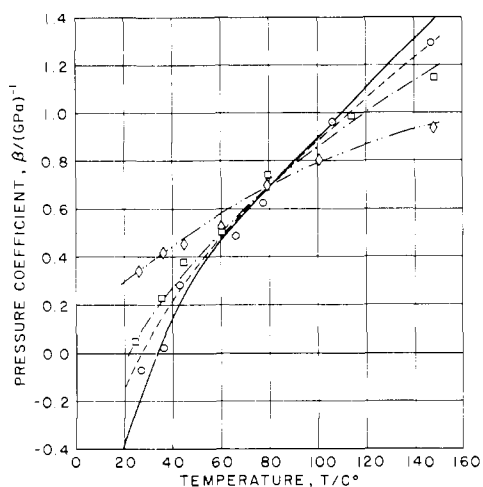


Figure 12. Comparison between the experimental (symbols) and calculated (lines) pressure coefficients: $c = 0.0000\text{ m}$, —; $c = 0.5027\text{ m}$, O, ---; $c = 1.4984\text{ m}$, □, -.-; $c = 4.3925\text{ m}$, ◇, -·-·-.

In the third stage, the pressure coefficient $\beta(T, c)$ was correlated in the manner described in ref 8 by means of the expressions given below.

$$\beta(T, c) = \beta_s^E(T)\beta^*(c/c_s) + \beta_w(T) \quad (11)$$

Here the superscript E refers to the excess pressure coefficient over that of pure water, $\beta_w(T)$, and the subscript s refers to KCl saturation conditions. The pressure coefficient for water in the temperature range 10–150 °C was given by Kestin et al. (9) as

$$\beta_w(T)/\text{GPa}^{-1} = -1.297 + 0.574 \times 10^{-1}(T/^\circ\text{C}) - 0.697 \times 10^{-3}(T/^\circ\text{C})^2 + 0.447 \times 10^{-5}(T/^\circ\text{C})^3 - 0.105 \times 10^{-7}(T/^\circ\text{C})^4 \quad (12)$$

The excess pressure coefficient at saturation, β_s^E , is given by

$$\beta_s^E(T)/\text{GPa}^{-1} = 0.241 + 0.478 \times 10^{-2}(T/^\circ\text{C}) - \beta_w(T) \quad (13)$$

whereas the saturation concentration, $c_s(T)$, was taken from a correlation of the data given in ref 16 and 19.

$$c_s(T)/\text{m} = 3.825 + 0.394 \times 10^{-1}(T/^\circ\text{C}) - 0.197 \times 10^{-4}(T/^\circ\text{C})^2 \quad (14)$$

Finally the reduced excess pressure coefficient β^* was calculated from

$$\beta^*(c/c_s) = \beta^E(T, c)/\beta_s^E(T) = 3.25(c/c_s) - 3.5(c/c_s)^2 + 1.25(c/c_s)^3 \quad (15)$$

Figure 12 shows a comparison between the experimental and calculated values of the pressure coefficients for three concentrations: $c = 0.5027\text{ m}$, $c = 1.4984\text{ m}$, and $c = 4.3925\text{ m}$; the pressure coefficient for pure water represented by eq 12 is shown as a solid line. It can be seen that the correlation represents the pressure coefficient to within their expected uncertainty, i.e., $\pm 25\%$, which is adequate for our purposes.

The correlation represented by eq 9–15 reproduces the entire body of experimental results (Tables V–IX) to within a standard deviation of $\pm 0.6\%$. Figure 13 depicts the deviations of the experimental points from the correlation. The highest deviations

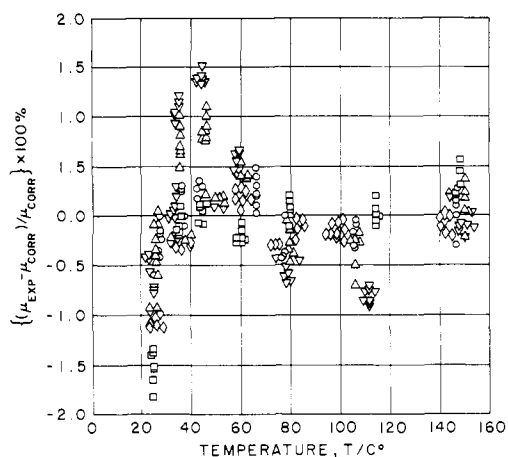


Figure 13. An overall comparison between the present experimental results and the correlation $\mu(P, T, c)$: O, $c = 0.5027\text{ m}$; □, $c = 1.4984\text{ m}$; Δ, $c = 2.5039\text{ m}$; ▽, $c = 3.5010\text{ m}$; ◇, $c = 4.3925\text{ m}$.

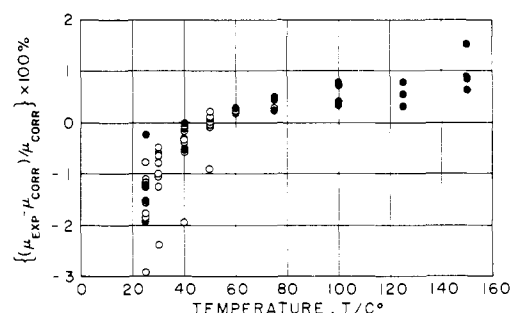


Figure 14. Comparison between the experimental results of Goncalves and Kestin (5), those of Korosi and Fabuss (14), and the present correlation: O, Goncalves and Kestin (5); ●, Korosi and Fabuss (14).

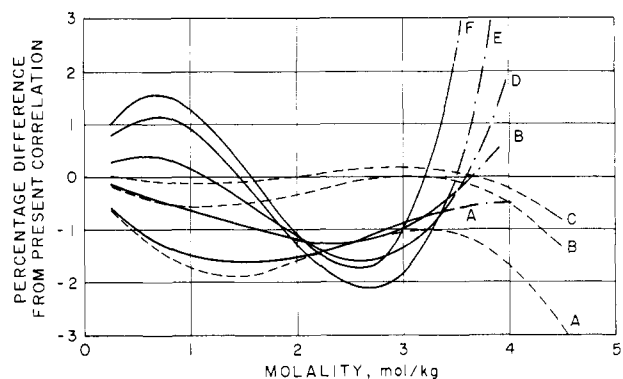


Figure 15. Comparison between the correlations of ref 5 and 14 and the present one: ---, Goncalves and Kestin (5); —, Korosi and Fabuss (14).

occur in the low-temperature region but never exceed 1.8%. The deviations are generally within the estimated accuracy of the experimental data ($\pm 1\%$).

6. Comparison with Other Results

A careful search of available literature references (18) has revealed that measurements of the viscosity of KCl solutions are, more or less, confined to atmospheric pressure, low temperatures, and low concentrations. The only exceptions can be found in the work of Korosi and Fabuss (14) and Goncalves and Kestin (5). Korosi and Fabuss (14) measured over the temperature range 25–150 °C and the concentration range 0–3.5 m, whereas the measurements of Goncalves and Kestin (5) were limited to the temperature range 20–50 °C but covered

the wide concentration range 0–4.6 *m*. The deviation plot of Figure 14 displays the comparison between the measurements of Korosi and Fabuss (14) and the present correlation. The maximum deviation is about 1.8% and the standard deviation is $\pm 1.0\%$ which is within the mutual uncertainty. Figure 14 also displays the corresponding comparison for the measurements of Goncalves and Kestin (5). Here the correlation predicts values that are consistently higher than the measurements with a maximum absolute deviation of 2.9% and a standard deviation of about $\pm 1.1\%$, again within the mutual uncertainty.

Figure 15 shows a comparison between the correlations given in ref 5 and 14 and the present correlation in the temperature and concentration ranges where the correlations apply, i.e., 25–150 °C and 0–3.5 *m* for ref 14 and 25–50 °C and 0–4.6 *m* for ref 5. The lines exhibit the same general behavior as the experimental points shown in Figure 14.

Acknowledgment

The authors thank Mr. R. Correia for helping with some of the calculations and to Dr. J. L. Haas, Jr., for his helpful suggestions.

Literature Cited

- (1) Bell, J. T., Helton, D. M., Rogers, T. G., *J. Chem. Eng. Data*, **15**, 44 (1970).
- (2) Egorov, V. Ya., Zarembo, V. I., Fedorov, M. K., *Zh. Prikl. Khim. (Leningrad)*, **49**, 124 (1976).
- (3) Ellis, A. J., *J. Chem. Soc. A*, 1579 (1966).

- (4) Gibson, R. E., *J. Am. Chem. Soc.*, **57**, 284 (1935).
- (5) Goncalves, F. A., Kestin, J., *Ber. Bunsenges. Phys. Chem.*, **81**, 1156 (1977).
- (6) Kell, G. S., Whalley, E., *J. Chem. Phys.*, **62**, 3496 (1975).
- (7) Kestin, J., Khalifa, H. E., *Appl. Sci. Res.*, **32**, 483 (1976).
- (8) Kestin, J., Khalifa, H. E., Abe, Y., Grimes, C. E., Sookiazian, H., Wakeham, W. A., *J. Chem. Eng. Data*, **23**, 328 (1978).
- (9) Kestin, J., Khalifa, H. E., Sookiazian, H., Wakeham, W. A., *Ber. Bunsenges. Phys. Chem.*, **82**, 180 (1978).
- (10) Kestin, J., Leidenfrost, W., Liu, C. Y., *Z. Angew. Math. Phys.*, **10**, 558 (1959).
- (11) Kestin, J., Moszynski, J. R., *Trans. ASME*, **80**, 1009 (1958).
- (12) Kestin, J., Sokolov, M., Wakeham, W. A., *J. Phys. Chem. Ref. Data*, **7** (3) (1978).
- (13) Kestin, J., Wang, H. E., *J. Appl. Mech.*, **79**, 197 (1957).
- (14) Korosi, A., Fabuss, B. M., *J. Chem. Eng. Data*, **13**, 548 (1968).
- (15) Mikhailov, I. G., Shutilov, V. A., *Akust. Zh.*, **10**, 450 (1964).
- (16) Potter, R. W., II, Babcock, R. S., Brown, D. L., *J. Res. U.S. Geol. Surv.*, **5**, 389 (1977).
- (17) Potter, R. W., II, Brown, D. L., *U.S. Geol. Surv.* (open file report), **No. 76-243** (1976).
- (18) Potter, R. W., II, Shaw, D. R., Haas, J. L., Jr., *U.S. Geol. Surv., Bull.*, **No. 1417** (1975).
- (19) Seidell, A., "Solubilities of Inorganic and Metal Organic Compounds", Vol. 1, Van Nostrand, New York, 1940.
- (20) Swindells, J. F., Coe, J. R., Jr., Godfrey, T. B., *J. Res. Natl. Bur. Stand.*, **48**, 1 (1952).
- (21) Vaslow, F., *J. Phys. Chem.*, **70**, 2286 (1966).

Received for review July 28, 1978. Accepted December 4, 1978. The work described in this paper has been performed under the sponsorship of the United States Geological Survey, Contract No. 14-08-0001-G-342 awarded to Brown University.

Supplementary Material Available: Figures 6–10, which display the viscosity of the five solutions as a function of pressure along various isotherms (5 pages). Ordering information is given on any current masthead page.

Solubility of Metal Sulfides in Sodium Polysulfide Melts

Ronald A. Bailey* and James M. Skeaff

Department of Chemistry, Rensselaer Polytechnic Institute, Troy, New York 12181

The solubilities of six transition metal sulfides are reported in Na_2S_x melts over the composition range $\text{Na}_2\text{S}_{2.7}$ to Na_2S_5 , at temperatures of 275–375 °C. The apparatus for these solubility measurements is described.

The use of sodium polysulfide melts in the sodium–sulfur battery, and the solubility behavior of metal sulfides that are potential corrosion products in some designs, led to our making solubility measurements in several such systems. Primarily, we have considered solubility as a function of polysulfide composition, which is of interest over the range Na_2S_2 to Na_2S_5 .

Experimental Section

Measurement of solubilities in molten polysulfides is complicated by the volatility of sulfur from the melt with consequent compositional changes. The cell used is illustrated in Figure 1. A product with the approximate composition Na_2S_3 was prepared by the method of Cleaver et al. (1). Other compositions were prepared by adding additional sulfur to this. Approximately 5 g of Na_2S_x and the metal sulfide were placed in the side arm through the port B. The cell was evacuated, entrance port B sealed, and the cell placed in the furnace. Any sulfur vapor condensed in the cold part of the capillary tube that extends out of the furnace; in practice only a small amount was evolved. After equilibrium was achieved (7 days were allowed, with occasional shaking) the cell was inverted to let the melt rest

Table I. Equilibrium Solubilities of Some Metal Sulfides in Sodium Polysulfide Melts

melt compn	temp, °C	solubility					
		Cr_2S_3 , $\mu\text{g/g}$	MnS , mg/g	FeS , mg/g	NiS , mg/g	CuS , mg/g	Cu_2S , mg/g
$\text{Na}_2\text{S}_{2.74}$	375	6.0	0.50	3.99	4.64		
$\text{Na}_2\text{S}_{2.9}$	300			2.0	0.8		
Na_2S_3	275					24.3	10.5
$\text{Na}_2\text{S}_{3.2}$	375	40.6	1.18	2.72	1.18		
Na_2S_4	375	46.2	2.12	1.28	0.47		
Na_2S_4	325	30.0		0.6			
Na_2S_5	375	71.4	3.42	0.17	0.15		
Na_2S_5	300			0.1	0.1		
Na_2S_5	275					106.5	40.5

on the frit and replaced in the furnace, and the capillary tube opened to vacuum to initiate filtration through the frit. The sulfur vapor lost in this way was negligible in the time required for filtration. After cooling, the cell was broken open and the dissolved metal content in the Na_2S_x determined by atomic absorption spectroscopy after dissolution in acid. Most solubilities were such that dilutions of the order of 1 g of $\text{Na}_2\text{S}_x/\text{L}$ were in the appropriate range, so that generally the dilution steps necessary for the atomic absorption analyses did not introduce excessive error into the measurements. The Na_2S_x composition was determined from the weight of NaCl formed when an aqueous solution of the melt was treated with HCl , filtered, and evaporated to dryness.